UDK 669.14.018:621.791.05:539.42
Original scientific article/Izvirni znanstveni članek

ISSN 1580-2949
MTAEC9, 42(6)263(2008)

EXPERIMENTAL ANALYSIS OF CRACK INITIATION AND GROWTH IN WELDED JOINT OF STEEL FOR ELEVATED TEMPERATURE

EKSPERIMENTALNA ANALIZA NASTANKA IN RASTI RAZPOKE V ZVARU JEKLA ZA POVIŠANO TEMPERATURO

Meri Burzić[1], Živoslav Adamović[2]

[1] Institute "GOŠA", d. o. o., Milana Rakića 35, 11000 Belgrade, Serbia
[2] University of Novi Sad, "Mihajlo Pupin" Faculty of Technical Engineering, Đure Đakovića bb, 23000 Zrenjanin, Serbia
merib@neobee.net

Prejem rokopisa – received: 2008-07-10; sprejem za objavo – accepted for publication: 2008-07-22

This paper presents results of experimental investigation of crack resistance by static and variable loading of alloyed steel A-387 Gr. 11 for elevated temperature application and its welded joint. Using SEN-B, CT and Charpy pre-cracked specimens, the significance of heterogeneity of microstructure and mechanical properties of welded joints on fracture toughness and fatigue crack initiation and propagation, at room and working temperatures, is evaluated.

Keywords: alloyed steel, welded joint, fracture toughness, crack propagation rate, fatigue crack, fatigue threshold

V članku je predstavljena eksperimentalna raziskava odpornosti razpoke pri statični in izmenični obremenitvi pri jeklu A-387Gr 11 za uporabo pri povišani temperaturi in zvarih tega jekla. Z uporabo SEN-B-, CT- in Charpy-preizkušancev z razpoko smo ocenili pomen heterogenosti mikrostrukture in mehanskih lastnosti zvara za žilavost loma in za začetek ter za napredovanje utrujenostne razpoke pri sobni in pri delovni temperaturi.

Ključne besede: legirano jeklo, zvar, žilavost loma, hitrost napredovanja razpoke, prag utrujenosti

1 INTRODUCTION

The in-service behaviour of alloyed steel A-387 Gr. 11 Class 1, for pressure vessels, used for high temperature applications, depends on the properties of its welded joint, with parent metal (BM), heat-affected-zone (HAZ) and weld metal (WM) as constituents. Critical locations, regarding integrity of welded joint can be formed in HAZ and WM [1]. Qualification of specified welding technology of plates, 96 mm thick, of steel A-387 is performed according to standard EN 288-3 [2].

While determining the plane strain fracture toughness, K_{Ic}, of welded joint constituents with heterogeneous microstructure, one must bear in mind, in order to hold the validity of theoretical assumptions and meanings of fracture toughness as measured property, that fracture mechanics is based on material homogeneity, including the region of crack tip.

A characteristical property of the welded joint is the heterogeneity of microstructure and mechanical properties, together with, irregular internal stress distribution with residual stresses and stress concentration. These important problems do not exclude experimental determination of plane strain fracture toughness, K_{Ic}, of welded joint and its constituents, although they present difficulties in the interpretation of measured values and obtained results [3–5].

For better understanding of crack occurrence and its growth effect in welded joints of steel for elevated temperatures, applied in equipment for high pressure, it is necessary to quantify the parameters controlling the strain behaviour in crack tip vicinity and crack resistance. Therefore, in this paper the effect of heterogeneity of microstructure and mechanical properties on fracture toughness, K_{Ic}, fatigue crack growth rate, da/dN, and fatigue threshold stress intensity factor range, ΔK_{th}, of A-387 steel and its welded joint constituents is experimentally investigated at room temperature (20 °C) and at working temperature (540 °C) [6].

2 MATERIAL FOR TESTING

The welded joint sample (350 × 500 × 96) mm with double "U" weld metal in the middle of the steel A-387 was used for this investigation [6]. Two welding procedures were applied [6]:

- shielded metal manual arc welding (SMAW) with coated electrode LINCOLN Sl 19G (AWS: E8018-B2 for root weld passes;
- Submerged arc welding (SAW), applying as consumable wire LINCOLN LNS 150 and flux LINCOLN P230, for filler passes.

The welded sample and scheme of cutting out of specimens from welded joint (OM, HAZ and WM) are shown in **Figure 1**. The chemical composition and mechanical properties of A-387 1 steel are given in **Tables 1 and 2**. The chemical composition of electrode LINCOLN Sl 19G and wire LINCOLN LNS 150

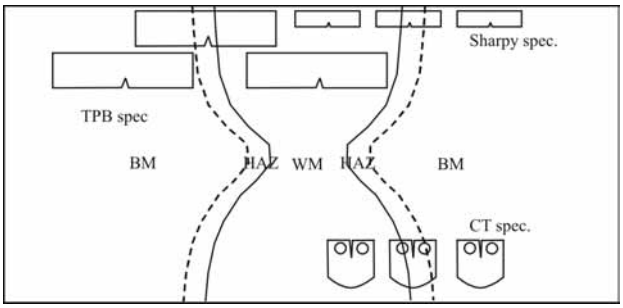

Figure 1: Scheme of testing sample of double "U" weld metal and specimens sampling [6]
Slika 1: Shema preizkušanca z dvojnim U-zvarom in odvzem vzorcev [6]

according to certificates is given in **Table 3**, and the mechanical properties according to certificates are given in **Table 4**.

Table 1: Chemical composition of tested steel A-387
Tabela 1: Kemična sestava jekla A-387, ki je bilo uporabljeno za preizkuse

Chemical composition, *w*/%						
C	Si	Mn	P	S	Cr	Mo
0.15	0.29	0.54	0.022	0.011	0.93	0.47

Table 2: Required mechanical properties of tested steel A-387
Tabela 2: Predpisane mehanske lastnosti za jeklo A-387

Yield stress, min.	Tensile strength	Elongation	Impact energy
$R_{p0,2}$/MPa	R_m/MPa	*A*/%	*KV*/J
315	490-620	25	> 85

Table 3: Chemical composition of filler metal [6]
Tabela 3: Kemična sestava deponiranega materiala [6]

Filler material	Chemical composition, *w*/%						
	C	Si	Mn	P	S	Cr	Mo
LINCOLN Sl 19G	0.08	0.045	0.35	0.025	0.025	1.10	0.50
LINCOLN LNS 150	0.11	0.18	0.37	0.020	0.020	1.04	0.47

Table 4: Mechanical properties of filler metal [6]
Tabela 4: Mehanske lastnosti deponiranega materiala [6]

Filler material	Yield stress $R_{p0,2}$/MPa	Tensile strength R_m/MPa	Elongation *A*/%	Impact energy *KV*/J
LINCOLN Sl 19G	505	640	23	> 95
LINCOLN LNS 150	490	610	26	> 100

3 TENSILE PROPERTIES

Tensile testing of specimens taken from parent metal, from weld metal, and from butt welded joint, were performed on an machine in displacement control, at room and at working temperature. The specimen from WM for testing at room temperature, was machined from

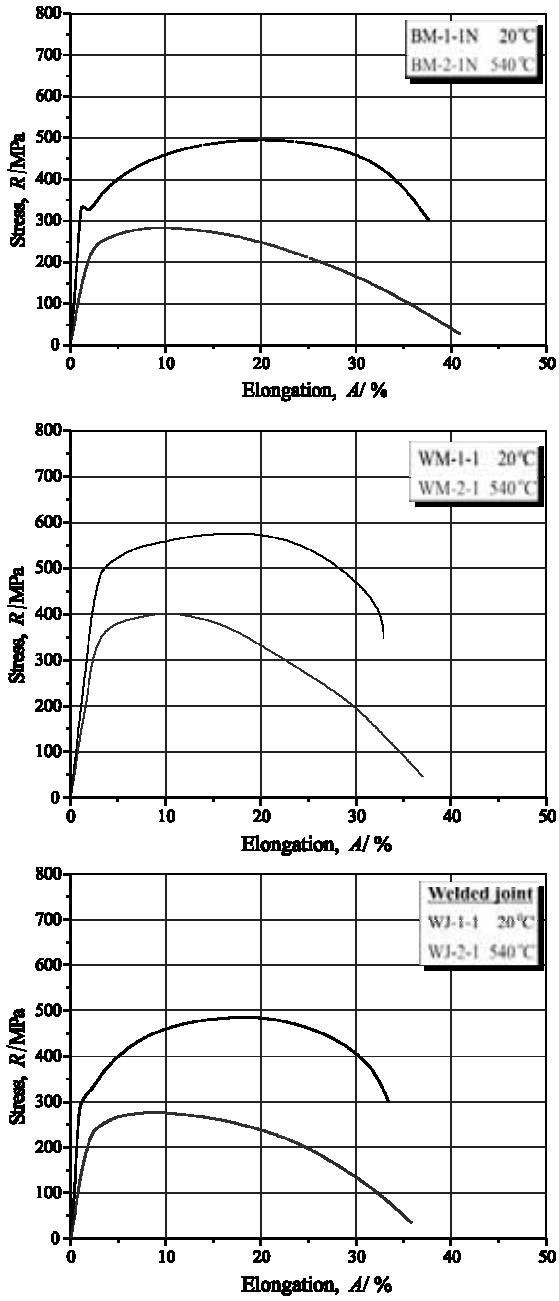

Figure 2: Diagrams stress – elongation: a) BM, b) WM, c) welded joint
Slika 2: Odvisnosti napetost–podaljšek: a) BM, b) WM, c) zvarni spoj

the available material, according to standard EN 895 [7]. For easier comparison of results the specimen from BM is of the same dimensions according the standard EN 10002-1 were used. Specimen from welded joint was made according EN 895. For testing at the temperature of 540 °C the same specimen design according to standard ASTM E1475-00 [8] was used for all welded joint consituents with dimensions adopted to available equipment.

Typical stress – strain curves for specimens from BM, WM and from welded joint, tested at room and

working temperature, are given in **Figure 2**. The testing results at room and at working temperatures are given in **Table 5** for BM, in **Table 6** for WM and in **Table 7** for the specimens of welded joint.

The effect of testing temperature on tensile properties is clear. At higher temperature the values of yield stress and tensile strength are smaller, and elongation values are increased, as seen in **Figure 2** and in **Tables 5–7** [7]. However, this conclusion is very simplified and apparent, as it will be discussed.

Table 5: Results of tensile testing of BM specimens
Tabela 5: Rezultati nateznih preizkusov BM-preizkušancev

Specimen	Testing temperature °C	Yield stress $R_{p0,2}$/MPa	Tensile strength R_m/MPa	Elongation A/%
OM-1-1N	20	330	495	37.6
OM-1-2N		318	479	36.1
OM-1-3N		324	488	38.7
OM-2-1N	540	219	284	40.1
OM-2-2N		212	279	39.6
OM-2-3N		226	303	39.9

Table 6: Results of tensile testing of WM specimens
Tabela 6: Rezultati nateznih preizkusov WM-preizkušancev

Specimen	Testing temperature °C	Yield stress $R_{p0,2}$/MPa	Tensile strength R_m/MPa	Elongation A/%
OM-1-1N	20	491	576	32.7
OM-1-2N		504	592	31.6
OM-1-3N		496	585	33.9
OM-2-1N	540	338	401	36.9
OM-2-2N		331	396	36.2
OM-2-3N		345	409	37.8

Table 7: Results of tensile testing of welded joint specimens
Tabela 7: Rezultati nateznih preizkusov WM-preizkušancev

Specimen	Testing tempe-rature °C	Yield stress $R_{p0,2}$/MPa	Tensile strength R_m/MPa	Elongation* A/%	Location of fracture
ZS – 1 – 1	20	322	488	33.5	BM
ZS – 1 – 2		319	497	32.2	BM
ZS – 1 – 3		315	491	31.9	BM
ZS – 2 – 1	540	221	278	35.8	BM
ZS – 2 – 2		224	285	34.6	BM
ZS – 2 – 3		217	277	37.9	BM

*measured at L_0 = 100 mm, as comparative value (is not material property)

The basic requirement in welded structures design is to assure the required strength. In most welded structures this is achieved with superior strength of WM compared to BM (overmatching effect). In tested case this is achieved at room and at working temperatures (**Figure 2 a, b, Tables 5, 6**). An additional proof of ovetmatching is the fracture of specimens from welded joint in BM and that the difference of values of yield stress and tensile strength in **Tables 5 and 7** is minor, at the level of measurement error. It is to notice the good agreement between yield stress and tensile strength values from test (**Table 5**) and specified values (**Table 2**). The obtained results of tensile properties of WM, **Table 6** and **Figure 4b**, confirmed that welding technology was properly specified (welding procedure specification – WPS – is a separate document), including preheating and post-weld heat treatment.

Special attention in tensile properties should be paid to elongation. When material is homogenious, as here BM and WM should be considered, elongation is usefull for comparison. For welded joint, the elongation value is meaningless, since in measuring length of 100 mm enter BM i WM, of different tensile properties, but also a part of HAZ is included, in which tensile properties are unknown. Nevertheless, the character of obtained tensile curves shows that material is ductile and it has an approximate ratio of unifirom and non-uniform elongation 1 : 2 (**Figure 2**). From the aspect of in-service behaviour of the welded structure, it is to underline that for real values elongation is elastic, and only locally and in limited amount also plastic, so the elongation values from **Figure 2 and Tables 5–7** can serve only for comparison and can not be the base for material behaviour assessment, especially HAZ, occurrence and crack propagation.

In the performed test, of special importance is that the obtained strength values at the working temperature are within specified levels. This will significantly contribute to crack resistance evaluation of the statically and variably loaded heterogenious structure, such as welded joint and heat-affected-zone are.

4 EXAMINATION OF MICROSTRUCTURE

A macrograph of butt welded joint of A-387 steel is given in **Figure 3**. Clearly recognized are: parent metal (BM) and weld metal (WM), and also heat-affected-zone (HAZ) in between [6].

Figure 3: Macrograph of welded joint
Slika 3: Makroposnetek zvarnega spoja

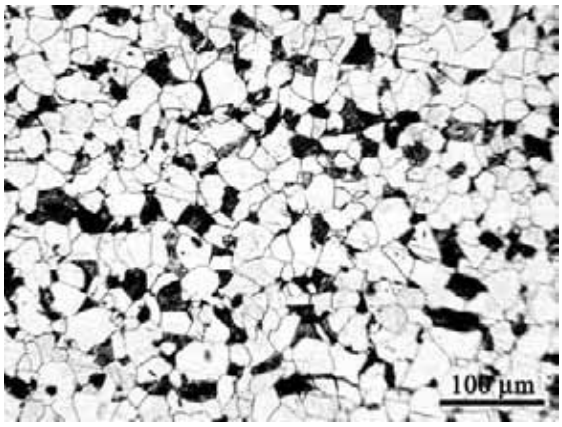

Figure 4: Microstrukture of parent metal (BM)
Slika 4: Mikrostruktura osnovnega materiala

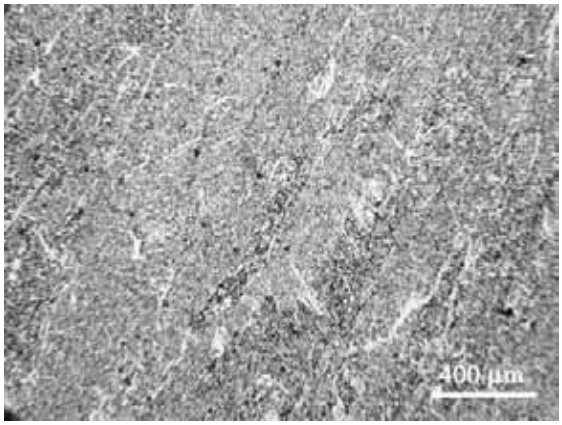

Figure 5: Microstrukture of weld metal (WM)
Slika 5: Mikrostruktura vara

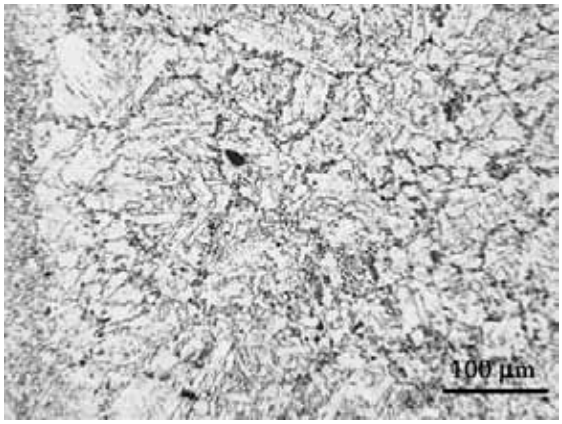

Figure 6: Microstrukture of the heat-affected-zone (HAZ)
Slika 6: Mikrostruktura toplotne zone

The uniform microstructure of parent metal, in addition to light polygonal crystals of ferrite, contains of pearlite as polygonal dark micro-constituent. The BM microstructure is presented in **Figure 4** with solidification grain size 5 according to ASTM [6]. The weld metal microstructure is bainite and grain boundary ferrite, **Figure 5** [6]. HAZ microstructure comprises from coarse grained bainite which is located next to the WM and fine grained bainite, next to the BM, **Figure 6** [6]. One has to have in mind that this local microstructure can significantly differ from microstructures at other locations in HAZ.

5 FRACTURE TOUGHNESS TESTING

The effect of microstructure and mechanical properties heterogeneity of welded joint constituents on the plane-strain fracture toughness, K_{Ic}, can be assessed locating a fatigue pre-crack tip on the specimen in different regions and following the regions of fracture growth.

5.1 Procedure and testing results

Fracture toughness testing were performed using three-points bend, 17.5 mm thick specimens (SEN-B), **Figure 7a**, and 8 mm thick, compact tension specimens (CT), **Figure 7b** to according the standard ASTM E1820 [9]. Three-point bend (SEN-B) specimens were tested at room temperature. Only CT specimens were tested at working temperature.

Fracture toughness, K_{Ic}, a measure of fracture toughness, J_{Ic}, is determined based on J-integral critical value, by testing according to ASTM E813-89 standard [10]:

$$K_{Ic} = \sqrt{\frac{J_{Ic} \cdot E}{1-\nu^2}} \qquad (1)$$

where: E – elasticity modulus, and ν – Poisson's ratio.

For the determination of the J-integral a single specimen testing method by successive partial unloading was applied. By data pairs applied force, F, – crack opening displacement, δ, the points of basic relationship curve were obtained (**Figure 8**, left). The procedure for the determination of critical value, as measure of the fracture toughness, J_{Ic}, requires the design of resistance curve (J-R curve), shown in **Figure 8**, right, in which

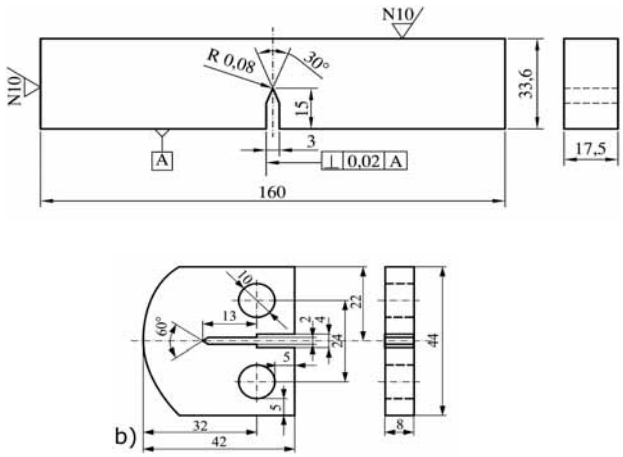

Figure 7: Specimen for fracture mechanic testing: **a)** SEN-B specimen, **b)** CT specimen
Slika 7: Preizkušanci za preizkuse mehanike loma: **a)** SEN-B, **b)** CT

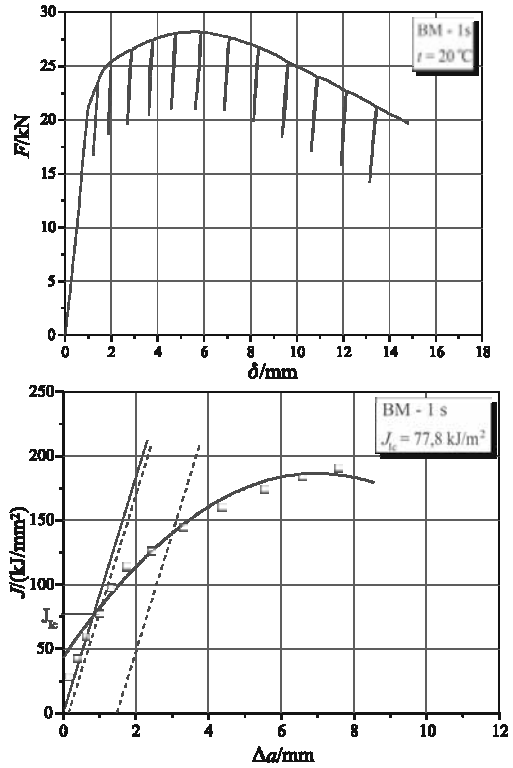

Figure 8: Diagrams $F - \delta$ (a) and $J - \Delta a$ (b) for the specimen with a notch in BM for room temperature

Slika 8: Odvisnosti $F - \delta$ (a) in $J - \Delta a$ (b) za preizkušanec z razpoko v BM pri sobni temperaturi

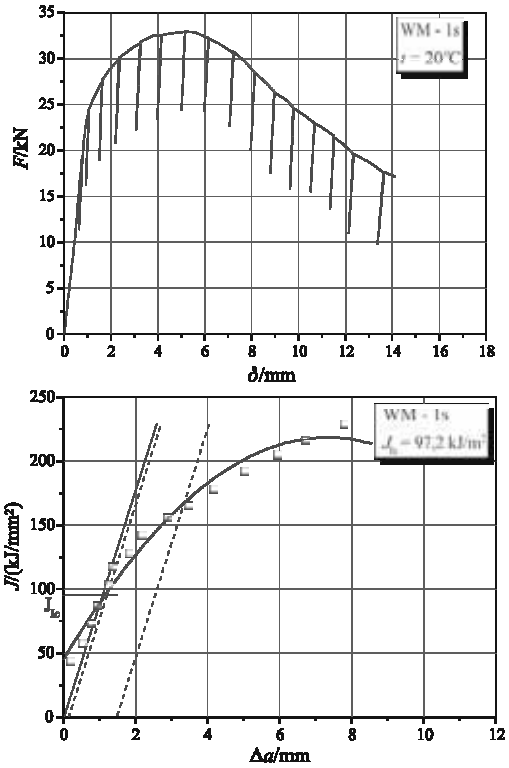

Figure 10: Diagrams $F - \delta$ (a) and $J - \Delta a$ (b) for the specimen with a notch in WM for room temperature

Slika 10: Odvisnosti F – δ (a) in $J - \Delta a$ (b) za preizkušanec z razpoko v WM pri sobni temperaturi

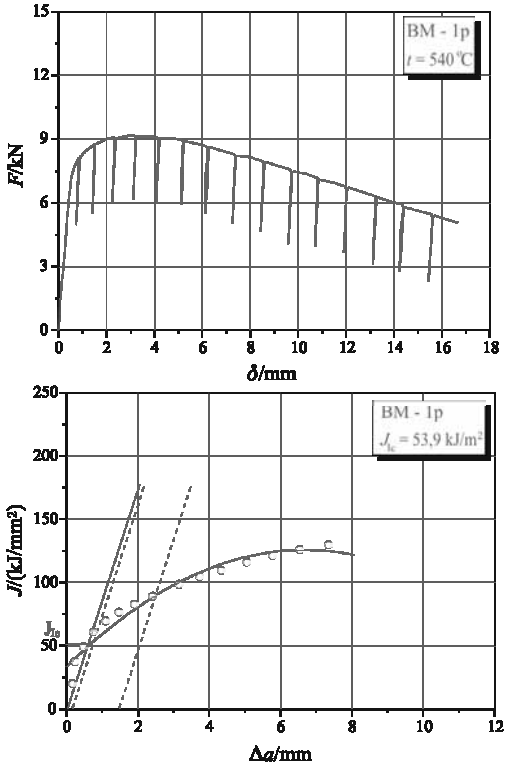

Figure 9: Diagrams $F - \delta$ (a) and $J - \Delta a$ (b) for the specimen with a notch in BM for operating temperature

Slika 9: Odvisnosti $F - \delta$ (a) in $J - \Delta a$ (b) za preizkušanec z razpoko v BM pri delovni temperaturi

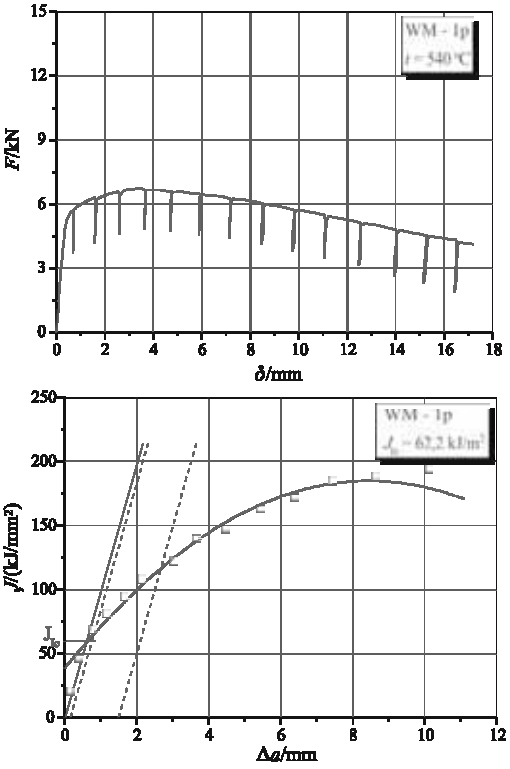

Figure 11: Diagrams $F - \delta$ (a) and $J - \Delta a$ (b) for the specimen with a notch in WM for operating temperature

Slika 11: Odvisnosti $F - \delta$ (a) in $J - \Delta a$ (b) za preizkušanec z razpoko v WM pri delovni temperaturi

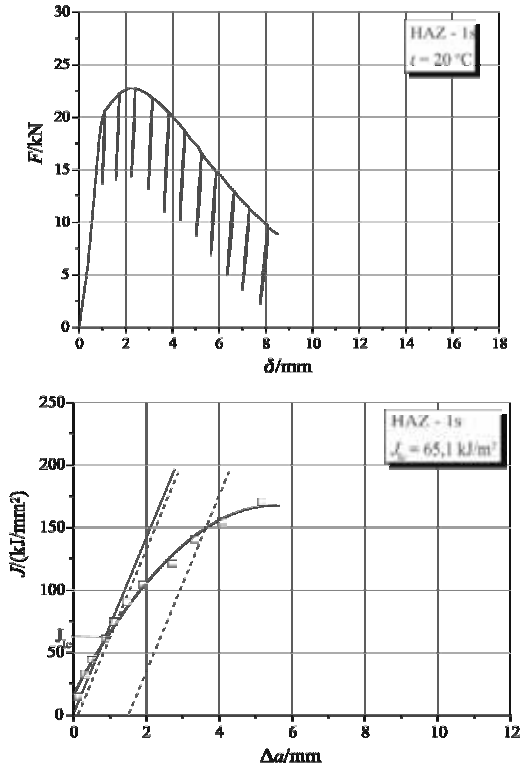

Figure 12: Diagrams $F - \delta$ (a) and $J - \Delta a$ (b) for the specimen with a notch in HAZ for room temperature

Slika 12: Odvisnosti $F - \delta$ (a) in $J - \Delta a$ (b) za preizkušanec z razpoko v HAZ pri sobni temperaturi

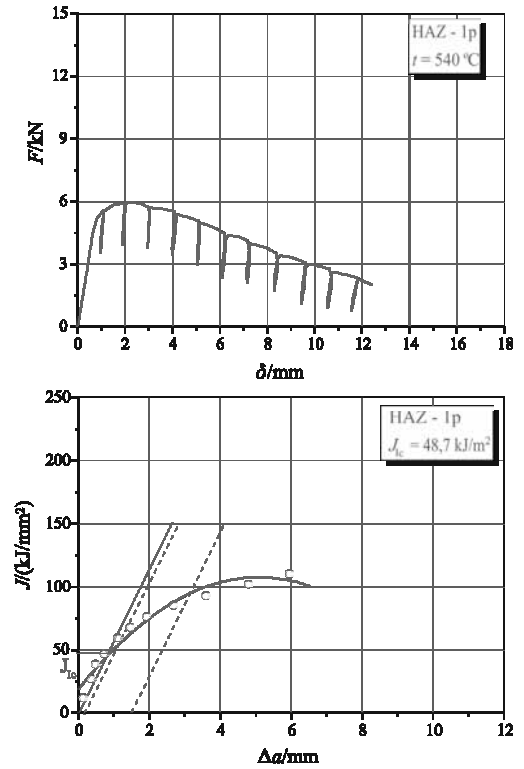

Figure 13: Diagrams $F - \delta$ (a) and $J - \Delta a$ (b) for the specimen with a notch in HAZ for operating temperature

Slika 13: Odvisnosti $F - \delta$ (a) in $J - \Delta a$ (b) za preizkušanec z razpoko v HAZ pri delovni temperaturi

crack increase is determined based on compliance change. Basic, but more expensive, is the procedure in ASTM E813 standard with the multi specimens (of the same size) method with different length of fatigue pre-crack, and different compliance.

In a single specimen test, the specimen is unloaded in intervals to about 30 % of the actually attained level of force chosen by experience with the type of material. Based on the change of line slope of the compliance, C, with crack extension, the crack increase, Δa, between two successive unloadings, corresponding to the attained value of force, is determined as:

$$\Delta a_i = \Delta a_{i-1} + \left(\frac{b_{i-1}}{\eta_{i-1}}\right) \cdot \left(\frac{c_i - c_{i-1}}{c_{i-1}}\right) \qquad (2)$$

The next steps are the determination of critical value, J_{Ic}, and use of this value in Eq. (1) for the calculation of the fracture toughness, K_{Ic}, according the single specimen compliance method.

5.2 Discussion of fracture toughness testing results

The obtained diagrams are presented in **Figure 8** for specimens of BM tested at room temperature and in **Figure 9** for specimens tested at 540 °C. The corresponding curves for WM are given in **Figures 10 and 11**, and for HAZ in **Figures 12 and 13** [6,11]. The calculated values of fracture toughness, K_{Ic}, are given in **Table 8** for the specimens notched in BM, WM and HAZ.

The microstructural and mechanical heterogeneities of a welded joint affect its resistance to crack propagation. Therefore, in specification for fracture mechanics testing conditions should prescribe not only the test procedure and location of a fatigue crack, but also the method of interpretation and meaning of the obtained results [6].

The character of curves varies depending on the notch i.e. fatigue crack, tip location and testing temperature. It is possible to observe an almost identical character of individual curves in each group, the difference between the diagrams for individual specimens lies exclusively in the maximal force value, F_{max}, which is directly dependent on the fatigue crack length, a, and on testing temperature [6].

The maximal value of K_{Ic} at room temperature was obtained for specimens notched in WM (mean K_{Ic} value $\approx$145 MPa m$^{1/2}$). Somewhat lower K_{Ic} values exhibited the specimens notched in BM (mean value K_{Ic} $\approx$130 MPa m$^{1/2}$). The scatter of results is small, 10–15 MPa m$^{1/2}$ in terms of minimum and maximum values. Lower K_{Ic} values belong to specimens notched in HAZ. The differences do not indicate an important reduction of properties [6]. The close K_{Ic} values for BM and HAZ are related to the microstructure. Namely, both constituents have ferrite-pearlite microstructures of similar crack resistance at static loading. It should be next in mind that in performed testing the location of fatigue crack tip is a

random one, and that in HAZ can exist the regions of different microstructure and lower fracture toughness.

Table 8: Results of testing the critical *J*-integral, J_{Ic}, and the critical stress intensity factor, K_{Ic}

Tabela 8: Rezultati preizkusa kritičnega *J*-integrala, J_{1c} in kritičnega faktorja intenzitete napetosti K_{IC}

Desig-nition	Testing tempera-ure °C	Critical J-integral J_{Ic}/(kJ/m^2)	Critical stress intensity factor, K_{Ic}/(MPa m$^{1/2}$)	Critical crack length a_c/mm
BM-1s	20	77.8	132.4	52.8
BM-2s		75.2	130.3	51.1
BM-3s		73.2	128.4	49.7
BM-1p	540	53.9	90.2	46.1
BM-2p		49.7	87.4	43.4
BM-3p		55.1	92.1	48.1
WM-1s	20	97.2	148.0	66.0
WM -2s		93.7	145.3	63.6
WM -3s		92.2	143.1	61.7
WM -1p	540	62.2	97.8	54.3
WM -2p		60.3	96.3	52.6
WM -3p		55.6	92.5	48.5
HAZ-1s	20	65.1	121.1	44.2
HAZ -2s		70.2	125.2	47.4
HAZ -3s		71.3	125.6	47.9
HAZ -1p	540	48.7	86.6	42.5
HAZ -2p		46.8	85.2	41.6
HAZ -3p		47.3	85.9	42.2

By applying the fundamental formula of fracture mechanics:

$$K_{Ic} = \sigma\sqrt{\pi \cdot a_c} \tag{3}$$

and introducing the value of allowable stress $\sigma_{doz} = \sigma$, for the shape factor equals to unity, approximate values of critical crack length, a_c, can be calculated, (**Table 8**). Largest crack length, a_c, can occur under static load in WM, but without brittle fracture occurrence.

For static loading, the given differences in K_{Ic} value should not have significant effect on structural safety. It is obvious that allowable stress, lower than yield stress, will produce higher values for critical crack length and if in the tested material the crack of length less than critical, there is no danger of brittle fracture. Such a crack has to be detected and its length assessed by convenient non-destructive testing method. After the integrity analysis it is possible, under defined conditions, allow for structure service even in crack growth period. Important data for a decision about the extended service of cracked component are crack growth rate and its dependance on applied load. The chages of K_{Ic} value are then important, since critical crack length, a_c, is directly depended on K_{Ic} value.

The effect of temperature on fracture toughness K_{Ic}, is given in **Table 8**. The reduction of 35–45 % in fracture toughness at working temperature compared to room temperature depends on fatigue crack tip location (BM, WM, HAZ), with maximum value of K_{Ic} in the specimen notched in WM. Obtained $J - \Delta a$ curves are of almost identical character, only the value of maximum force F_{max}, is different, and it is directly related to the fatigue crack length a.

5.3 Fatigue analysis by fracture mechanics

If a structural component is continuously exposed to variable loads, fatigue crack may initiate and propagate from severe stress raisers if the stress intensity factor range at fatigue threshold, ΔK_{th}, is exceeded.

A basic contribution of fracture mechanics in fatigue analysis is the division of fracture process to crack initiation period and the growth period to critical size for fast fracture. The total number of cycles to fracture, N_u, is divided into number of cycles for fatigue crack initiation, N_i, and for its growth to the value critical for fracture, N_p: ($N_u = N_i + N_p$)

The development in the research of material behaviour for variable loading is achieved applying experimental and theoretical approaches. The analysis of stress and strain state at growing fatigue crack tip by applying linear elastic fracture mechanics (LEFM) enabled to develop the Paris equation for metals and alloys, which relates fatigue crack growth rate da/dN to stress intensity factor range ΔK through coefficient C and exponent m [12]:

$$\frac{da}{dN} = C(\Delta K)^m \tag{4}$$

The standard ASTM E647 [13] defines the testing of pre-cracked specimen for fatigue crack growth rate measurement, da/dN, and for the calculation of the stress intensity factor range, ΔK. Two basic requirements in ASTM E647 are: the crack growth rate should be above 10^{-8} m/cycle to avoid fatigue threshold region and load should be of constant amplitude.

Standard Charpy size specimen, fatigue pre-cracked in different welded joint constituents, and instrumented by foil RUMUL RMF A-5, of measuring length 5 mm (**Figure 14**), for continuous monitoring of crack length, were tested at room temperature under variable loading for the determination of fatigue crack growth rate, da/dN, and stress-intensity factor range at fatigue threshold, ΔK_{th}. The testing was performed in load control, by

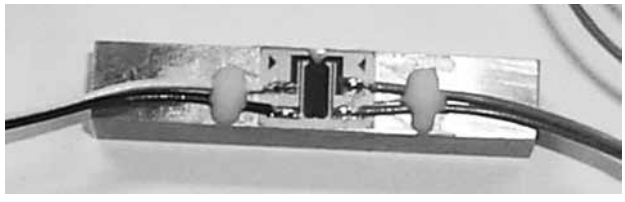

Figure 14: Charpy specimen instrumented by foil RUMUL RMF A-5 for continuous monitoring of crack length

Slika 14: Charpy preizkušanec s merilno folijo RUMUL RMF A-5 za zvezno merjenje dolžine razpoke

Table 9: Parameters of Paris equation
Tabela 9: Parametri Parisove enačbe

Specimen designation	Test temperature	Stress-intensity factor range at fatigue threshold	Coefficient	Exponent	Crack growth rate d*a*/d*N* at ΔK = 10 MPa $m^{1/2}$
	°C	ΔK_{th}/(MPa $m^{1/2}$)	*C*	*m*	nm/cycle
BM–1s	20	6.8	$2.98 \cdot 10^{-13}$	3.62	$1.24 \cdot 10^{-09}$
WM–1s		6.8	$3.88 \cdot 10^{-13}$	3.82	$2.56 \cdot 10^{-09}$
HAZ–1s		6.7	$3.05 \cdot 10^{-13}$	4.01	$3.12 \cdot 10^{-09}$
BM–1p	540	5.9	$3.11 \cdot 10^{-13}$	4.08	$3.74 \cdot 10^{-09}$
WM–1p		6.2	$3.27 \cdot 10^{-13}$	4.14	$4.51 \cdot 10^{-09}$
HAZ–1p		6.1	$3.38 \cdot 10^{-12}$	3.17	$5.00 \cdot 10^{-09}$

three-points bending on the FRACTOMAT high-frequency resonant pulsator.

CT specimens were tested on working temperature, since at 540 °C the measuring foils can not be used, and load line displacement is measured instead.

The relations d*a*/d*N* – ΔK are presented in **Figure 15** for the specimens pre-cracked in the parent metal (PM), in **Figure 16** for specimens pre-cracked in the weld metal (WM) and in **Figure 17** for specimens pre-cracked in the heat-affected-zone (HAZ). The values of coefficient *C* and exponent *m,* with the values of stress-intensity factor range at fatigue threshold, ΔK_{th}, are given in **Table 9**.

The dominant almost linear middle part of curve in **Figures 15–17** is covered by Paris law and is practically most important, since it allows to define the difference between fatigue crack low growth rates (initiation) close to fatigue threshold, and high rates (K_{Ic}), when fracture occurs. The application of Paris equation is very convenient for fatigue of structures produced of materials of elevated and high strength. As it can be seen from **Table 9**, the position of the fatigue crack-tip and the testing temperature significantly affect the ΔK_{th} values and the fatigue-crack growth [6]. For comparison of the properties of welded joint constituents the crack growth rates are calculated for different values of stress-intensity factor range ΔK. As a referent value ΔK

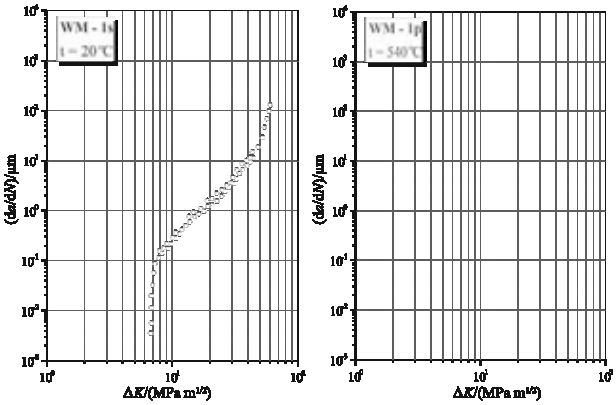

Figure 16: Fatigue crack growth rate per cycle, *da/dN*, vs. stress intensity factor range, ΔK, specimens pre-cracked in weld metal, tested at room temperature (left) and at 540 °C (right)
Slika 16: Rast utrujenostne razpoke na cikel d*a*/d*N* v odvisnosti od faktorja intenzitete napetosti ΔK, preizkušanec z razpoko v varku, preizkus pri sobni temperaturi (levo) in pri 540 °C (desno)

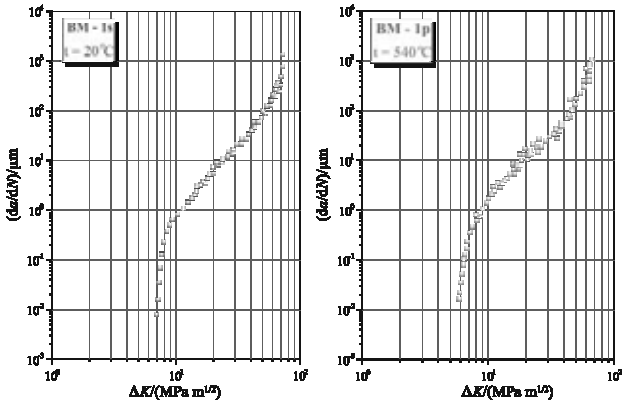

Figure 15: Fatigue crack growth rate per cycle, *da/dN*, vs. stress intensity factor range, ΔK, specimens pre-cracked in parent metal, tested at room temperature (left) and at 540 °C (right)
Slika 15: Rast utrujenostne razpoke na cikel d*a*/d*N* v odvisnosti od faktorja intenzitete napetosti ΔK, preizkušanec z razpoko v osnovnem materialu; preizkus pri sobni temperaturi (levo) in pri 540 °C (desno)

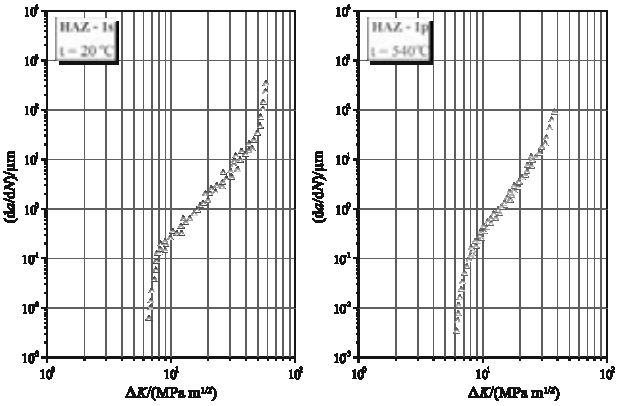

Figure 17: Fatigue crack growth rate per cycle, *da/dN*, vs. stress intensity factor range, ΔK, specimens pre-cracked in heat-affected-zone, tested at room temperature (left) and at 540 °C (right)
Slika 17: Rast utrujenostne razpoke na cikel d*a*/d*N* v odvisnosti od faktorja intenzitete napetosti ΔK, preizkušanec z razpoko v toplotni zoni, preizkus pri sobni temperaturi (levo) in pri 540 °C (desno)

= 10 MPa√m is accepted, which is within a middle part of the diagram, where Paris law is valid, **Figures 15–17**.

The fatigue crack-growth rate at room temperature, d*a*/d*N*, is $1.24 \cdot 10^{-09}$ μm/cycle for the specimen of BM, $2.56 \cdot 10^{-09}$ μm/cycle for specimen of WM and $3.12 \cdot 10^{-09}$ μm/cycle for specimen of HAZ At the temperature of 540 °C, corresponding values are higher: ($3.74 \cdot 10^{-09}$; $4.51 \cdot 10^{-09}$; $5.00 \cdot 10^{-09}$ for BM, WM and HAZ, in respect [6]. The behaviour of welded joint and its constituents should affect the change of curve slope in validity part of Paris law. Materials of lower fatigue-crack growth rate have lower slope in the diagram d*a*/d*N*\ *vs.* ΔK [6]. Slow growth is confirmed for specimens cracked in BM and WM, since for the same growth rate, greater factor intensity range is required. The maximum fatigue crack growth rate is expected when stress intensity factor range approaches to plane strain fracture toughness, when brittle fracture is possible [14].

In spite of significant differences in fatigue-crack growth rate, the obtained values are still low and acceptable. That means that tested steel and its welded joint exhibited acceptable level of fatigue-crack growth resistance and can be successfully applied for variable loading in case of detected crack-like defects, primarily for low-cycle fatigue.

6 CONCLUSIONS

The following conclusions were derived:

- The resistance to crack growth and obtained values of K_{Ic} and a_c of the welded joint are affected by its microstructural and mechanical heterogeneity and by the testing temperature. Feritte-lamelar pearlite microstructure of the WM has a better resistance to crack growth in static loading condition than the feritte-pearlite microstructure of BM of uniform grain size, and the feritte-pearlite microstructure of HAZ of different grain size. Obtained close K_{Ic} values of BM and HAZ are explained by the position of fatigue crack tip in HAZ region of the microstructure similar to that in BM.
- The testing temperature influences the fracture toughness K_{Ic} and the crack critical length a_{cr} values. The reduction of fracture toughness is of 35–45%, depending on fatigue crack tip location (BM, WM i HAZ). Specimen notched in WM has the highest value K_{Ic}, whereas for BM and HAZ obtained K_{Ic} values are lower. Results obtained at working temperature are proportionally lower compared to results at room temperature, and are a consequence of lower material properties at elevated temperature.
- Notch location and crack initiation, as well as testing temperature affect values of fatigue threshold ΔK_{th} and fatigue crack growth parameters.
- The minimum fatigue-crack growth rate exhibited the specimens pre-cracked in BM, and the maximum fatigue crack-growth rate in specimens pre-cracked in HAZ. This is directly connected to the effects that microstructural heterogeneity in HAZ regions has on fatigue-crack growth rate, d*a*/d*N*.
- Specimens of welded joint constituents at working temperature (540 °C) exhibited two to four-fold higher crack-growth rates when compared to room temperature under variable loads in tests of the fatigue threshold and fatigue crack growth parameters that this is explained by reduced material properties at elevated temperature.

7 REFERENCES

[1] S. Sedmak, A. Sedmak, Integrity of Penstcok of Hydroelectric Powerplant, Structural Integrity and Life, 5 (**2005**) 2, 59–70

[2] JUS EN 288-3:1992, Specification and approval of welding procedures for metallic materials – Part 3: Welding procedure tests for arc welding of steels, Službeni list SRJ, (**1995**), 25

[3] J. Vojvodic Tuma, A. Sedmak, Analysis of the unstable fracture behaviour of a high strength low alloy steel welment, Engineering Fracture Mechanics, 71 (**2004**), 1435–1451

[4] E. O. Argoub, A. Sedmak, M. A. Esasamei, Structural Integrity Assessment of Welded Plate with a Crack, Structural Integrity and Life, 4 (**2004**) 1, 39–46

[5] K. Gerić, PhD Thesis, University of Belgrade, Faculty of Tehnology and Metallurgy, Belgrade, 1997

[6] M. Burzić, PhD Thesis, University of Novi Sad, Technical faculty, 2008

[7] EN 895, Welded butt joints in metallic materials – Transverse tensile test, 1995

[8] ASTM E 1475-00, Standard Test Method for Measurement of Creep Crack Growth Rates in Metal, Annual Book of ASTM Standards 03.01.2000, 936–950

[9] ASTM E 1820-99a, Standard Test Method for Measurement of Fracture Toughness, Annual Book of ASTM Standards, 03.01, 1999

[10] ASTM E813-89, Standard Test Method for J_{Ic}, A Measure of Fracture Toughness, Annual Book of ASTM Standards, 03.01. 1993, 651

[11] M. Burzić, Z. Burzić, J. Kurai, The prediction of residual life of reactors in RNP, CertLab Pančevo, 2006

[12] P. C. Paris, F. Erdogan, A Critical Analysis of Crack Propagation Laws, Trans. ASME, Journal Basic Eng., 85, 4, 528

[13] ASTM E647, Standard Test Method for Constant-Load-Amplitude Fatigue Crack Growth Rates Above 10-8 m/cycle, Annual Book of ASTM Standards, 03.01. 1995, 714

[14] M. Burzić, Z. Burzić, J. Kurai, Dž. Gačo, Fatigue Behaviour of Alloyed Steel for High Temperature, First Serbian (26th YU) Congress on Theoretical and Applied Mechanics, Kopaonik, Serbia, 2007, 1085–1090